ISSN 1392 – 124X INFORMATION TECHNOLOGY AND CONTROL, 2006, Vol. 35, No. 4

DIRECT FIELD-ORIENTED CONTROL USING BACKSTEPPING STRATEGY WITH FUZZY ROTOR RESISTANCE ESTIMATOR FOR INDUCTION MOTOR SPEED CONTROL

Ismail Khalil Bousserhane, Abdeldjabbar Hazzab

University center of Bechar, B.P 417 Bechar 08000 Algeria

Mostefa Rahli, Mokhtar Kamli, Benyounes Mazari

University of Sciences and Technology of Oran, Algeria

Abstract. In this paper, the speed control of an induction motor using backstepping design with fuzzy rotor resistance estimation is proposed. First, the direct field oriented control IM is derived. Then, a backstepping for direct field oriented control is proposed to compensate the uncertainties, which occur in the control. Finally, a method of estimation of the rotor resistance in the backstepping control f induction motor drive. A model reference adaptive scheme is proposed in which the adaptation mechanism is executed using fuzzy logic. The effectiveness of the proposed control scheme is verified by numerical simulation. The numerical validation results of the proposed scheme have presented good performances compared to the conventional direct-field oriented control.

Keywords: induction motor, vector control, backstepping design, nonlinear control.

1. Introduction

Nowadays, like a consequence of the important progress in the power electronics and of micro-computing, the control of the AC electric machines known a considerable development and a possibility of the real time implantation applications. The Induction machine (IM) known by its robustness, cost, reliability and effectiveness is the subject of several researches [1]. However, it is traditionally for a long time, used in industrial applications that do not require high performances, this because of its high non-linearity and its high-coupled structure. On the other hand, the direct current (D.C) machine was largely used in the field of the variable speed applications, where torque and flux are naturally decoupled and can be controlled independently by the torque producing current and the flux producing current. Since Blashke and Hasse have developed the new technique known as vector control [1, 2, 3], the use of the induction machine becomes more and more frequent. This control strategy can provide the same performance as achieved from a separately excited DC machine, and is proven to be well adapted to all type of electrical drives associated with induction machines[4]. The vector control technique combines the slip calculation with a rotor-position or speed measurement [5]. The calculation of the slip speed in the direct vector control involves the rotor time constant, which may vary considerably over the operational range of the motor mainly due to changes in rotor resistance with temperature. An error in the slip speed calculation gives an error in the rotor flux position, resulting in coupling between the flux and torque-producing currents due to axis misalignment. This results in a torque response with possible overshoot or undershoot and a steady-state error. Therefore variations in motor parameters, particularly rotor resistance, should be tracked as they occur. For this reasons, many research have been done on automated tuning of induction motor parameters by various authors [5, 6, 7, 8].

The most widely used controller in the industrial applications is the PID-type controllers because of their simple structures and good performances in a wide range of operating conditions [9]. The PID controller's parameters are selected in an optimal way by known methods such as the Zeigler and Nichols, poles assignment... etc. However, the PID controllers are simple but cannot always effectively control systems with changing parameters or have a strong nonlinearity; and may need frequent on-line retuning [10].

Due to new developments in nonlinear control theory, several nonlinear control techniques have been introduced in the last two decades. One of the nonlinear control methods that has been applied to induction motor control is the backstepping design [11, 12]. The backstepping is a systematic and recursive design methodology for nonlinear feedback

control. This approach is based upon a systematic procedure for the design of feedback control strategies suitable for the design of a large class of feedback linearisable nonlinear systems exhibiting constant uncertainty, and guarantees global regulation and tracking for the class of nonlinear systems transformable into the parametric-strict feedback form. The backstepping design alleviates some of these limitations [11,13]. It offers a choice of design tools to accommodate uncertainties and nonlinearities and can avoid wasteful cancellations. The idea of backstepping design is to select recursively some appropriate functions of state variables as pseudo-control inputs for lower dimension subsystems of the overall system. Each backstepping stage results in a new pseudo-control design, expressed in terms of the pseudo-control designs from the preceding design stages. When the procedure terminates, a feedback design for the true control input results which achieves the original design objective by virtue of a final Lyapunov function, which is formed by summing up the Lyapunov functions associated with each individual design stage [14].

In this paper, we apply the backstepping technique to design a speed controller for the induction motor with fuzzy rotor resistance adaptation. The output of the backstepping controller is the current (i_{qs}) required to maintain the motor speed close to the reference speed. The current (i_{qs}) is forced to follow the control current by using current regulators. The direct field-oriented cnotrol of induction machine is presented in Section 2, the backstepping technique for IM control is summarized in Section 3. The proposed fuzzy estimation of the rotor resistance is derived in Section 4. Simulation results are reported in Section 5. Section 6 concludes the paper.

2. Direct field-oriented control of the IM

The dynamic model of three-phase, Y-connected induction motor can be expressed in the *d-q* synchronously rotating frame as [1, 14, 15]:

$$\begin{cases} \dfrac{di_{ds}}{dt} = \dfrac{1}{\sigma.L_s}\left(-\left(R_s+\left(\dfrac{L_m}{L_r}\right)^2.R_r\right).i_{ds}+\sigma.L_s.\omega_e.i_{qs}+\dfrac{L_m.R_r}{L_r^2}.\phi_{dr}+\dfrac{L_m}{L_r}.\phi_{qr}.\omega_r+V_{ds}\right) \\ \dfrac{di_{qs}}{dt} = \dfrac{1}{\sigma.L_s}\left(-\sigma.L_s.\omega_e.i_{ds}-\left(R_s+\left(\dfrac{L_m}{L_r}\right)^2.R_r\right).i_{qs}-\dfrac{L_m}{L_r}.\phi_{dr}.\omega_r+\dfrac{L_m.R_r}{L_r^2}.\phi_{qr}+V_{qs}\right) \\ \dfrac{d\phi_{dr}}{dt} = \dfrac{L_m.R_r}{L_r}.i_{ds}-\dfrac{R_r}{L_r}.\phi_{dr}+(\omega_e-\omega_r)\phi_{dr} \\ \dfrac{d\phi_{qr}}{dt} = \dfrac{L_m.R_r}{L_r}.i_{qs}-(\omega_e-\omega_r)\phi_{dr}-\dfrac{R_r}{L_r}.\phi_{qr} \\ \dfrac{d\omega_r}{dt} = \dfrac{P^2.L_m}{L_r.J}.(i_{qs}.\phi_{dr}-i_{ds}.\phi_{qr})-\dfrac{f_c}{J}.\omega_r-\dfrac{P}{J}.T_l \end{cases} \quad (1)$$

where σ is the coefficient of dispersion and is given by (2):

$$\sigma = 1-\frac{L_m^2}{L_s L_r} \quad (2)$$

L_s, L_r, L_m – stator, rotor and mutual inductances;

R_s, R_r – stator and rotor resistances;

ω_e, ω_r – electrical and rotor angular frequency;

ω_{sl} – slip frequency $(\omega_e-\omega_r)$;

τ_r – rotor time constant (L_r/R_r);

P – pole pairs.

The main objective of the vector control of induction motors is, as in DC machines, to independently control the torque and the flux; this is done by using a *d-q* rotating reference frame synchronously with the rotor flux space vector [2, 3]. In ideally field-oriented control, the rotor flux linkage axis is forced to align with the *d*-axes, and it follows that [3, 4, 16]:

$$\phi_{rq} = \frac{d\phi_{rq}}{dt} = 0\,, \quad (3)$$

$$\phi_{rd} = \phi_r = \text{constant}\,. \quad (4)$$

Applying the result of (3) and (4), namely field-oriented control, the torque equation becomes analogous to the DC machine and can be described as follows:

$$T_e = \frac{3}{2}\frac{p\cdot L_m}{L_r}\cdot\phi_r\cdot i_{qs}\,. \quad (5)$$

And the slip frequency can be given as follows:

$$\omega_{sl} = \frac{1}{\tau_r}\frac{i_{qs}^*}{i_{ds}^*}\,. \quad (6)$$

Consequently, the dynamic equations (1) yield:

$$\begin{cases} \dfrac{di_{ds}}{dt} = -\left(\dfrac{R_s}{\sigma L_s}+\dfrac{1-\sigma}{\sigma\tau_r}\right)i_{ds}+\omega_e i_{qs}+\dfrac{L_m}{\sigma L_s L_r\tau_r}\phi_{rd}+\dfrac{1}{\sigma L_s}V_{ds} \\ \dfrac{di_{qs}}{dt} = -\left(\dfrac{R_s}{\sigma L_s}+\dfrac{1-\sigma}{\sigma\tau_r}\right)i_{qs}-\omega_e i_{ds}+\dfrac{L_m}{\sigma L_s L_r\tau_r}\phi_{rd}+\dfrac{1}{\sigma L_s}V_{ds} \\ \dfrac{d\phi_r}{dt} = \dfrac{L_m}{\tau_r}i_{ds}-\dfrac{1}{\tau_r}\phi_{rd} \\ \dfrac{d\omega_r}{dt} = \dfrac{3}{2}\dfrac{P^2L_m}{JL_r}i_{qs}\phi_{rd}-\dfrac{f_c}{J}\omega_r-\dfrac{P}{J}T_l \end{cases} \quad (7)$$

Using (3) and (4) the desired flux in terms of i_{ds} can be found from:

$$\phi_{dr} = \frac{L_m/\tau_r}{s+1/\tau_r}\,. \quad (8)$$

The decoupling control method with compensation is to choose inverter output voltages such that [15]:

$$V_{ds}^* = \left(K_p+K_i\frac{1}{s}\right)\left(i_{ds}^*-i_{ds}\right)-\omega_e\sigma L_s i_{qs}^*\,, \quad (9)$$

$$V_{qs}^* = \left(K_p+K_i\frac{1}{s}\right)\left(i_{qs}^*-i_{qs}\right)+\omega_e\sigma L_s i_{ds}^*+\omega_r\frac{L_m}{L_r}\phi_{rd}\,. \quad (10)$$

According to the above analysis, the indirect field-oriented control (IFOC) [3, 15, 16] of induction motor with current-regulated PWM drive system can be

reasonably presented by the block diagram shown in Figure 1.

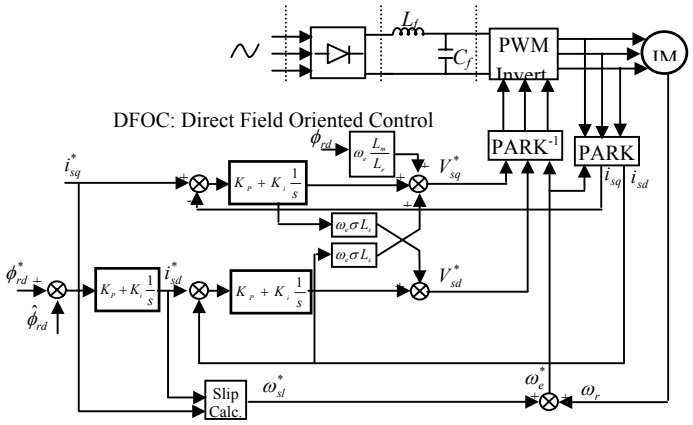

Figure 1. Block diagram of DFOC for an induction motor

3. The speed control of the IM using backstepping strategy

a) Backstepping technique

Consider the system :

$$\dot{x} = f(x) + g(x)u\ ,\ f(0) = 0\ , \tag{11}$$

where $x \in R^n$ is the state and $u \in R$ is the control input. Let $u_{des} = \alpha(x)$, $a(0) = 0$ be a desired feedback control law, which, if applied to the system in (11), guarantees global boundedness and regulation of $x(t)$ to the equilibrium point $x = 0$ as $t \to \infty$, for all $x(0)$ and $V(x)$ is a control Lyapunov function, where:

$$\frac{\partial V(x)}{\partial x}\left[f(x) + g(x)\alpha(x)\right] < 0\ ,\ V(x) > 0\ . \tag{12}$$

Consider the following cascade system :

$$\dot{x} = f(x) + g(x)y\ ,\ f(0) = 0\ , \tag{13}$$

$$\dot{\zeta} = m(x,\zeta) + \beta(x,\zeta)u\ ,\ h(0) = 0\ , \tag{14}$$

$$y = h(x)\ , \tag{15}$$

where for the system in (13), a desired feedback $a(x)$ and a control Lyapunov function *V(x)* are known. Then, using the nonlinear block backstepping theory in [17], the error between the actual and the desired input for the system in (13) can be defined as $z = y - \alpha$, and an overall control Lyapunov function $V(x,\zeta)$ for the systems in (13) and (14) can be defined by augmenting a quadratic term in the error variable z with $V(x)$:

$$V(x,\zeta) = V(x) + \frac{1}{2}z^2\ . \tag{16}$$

Taking the derivative of both sides gives:

$$\dot{V}(x,\zeta) = \dot{V}(x) + \frac{1}{2}z\dot{z} \tag{17}$$

From which solving for $u(x,\zeta)$, which renders $\dot{V}(x,\zeta)$ negative definite, yields a feedback control law for the full system in (13-15). One particular choice is (see [17]):

$$u = \left(\frac{\partial h(\zeta)}{\partial \zeta}\beta(x,\zeta)\right)^{-1}\left\{-c(y-\alpha) - \frac{\partial h(\zeta)}{\partial \zeta}m(x,\zeta) + \right. \tag{18}$$
$$\left. + \frac{\partial \alpha(x)}{\partial x}\dot{x} - \frac{\partial V(x)}{\partial x}g(x)\right\},\quad c > 0\quad .$$

b) Application to induction motor

In this section, we use the backstepping algorithm to develop a control law to regulate the speed of the induction motor. The speed will converge to its desired value from a wide set of initial conditions.

Step 1:

We first consider the tracking objective of the direct current (ϕ_{dr}). A tracking error $z_1 = \phi_{dr}^* - \phi_{dr}$ is defined and the derivative becomes:

$$\dot{z}_1 = \frac{d\phi_{dr}^*}{dt} - \frac{R_r}{L_r}\cdot\left(L_m \cdot i_{ds} - \phi_{dr}\right)\ . \tag{19}$$

To initiate backstepping, we choose i_{ds} as our first virtual control. If the stabilising function is chosen as:

$$i_{ds}^* = \frac{\phi_{dr}}{L_m} + c_1 \cdot \frac{\tau_r}{L_m}\cdot z_1 + \tau_r \cdot \frac{d\phi_{dr}}{dt}\ . \tag{20}$$

We obtain:

$$\dot{z}_1 = c_1 \cdot z_1 + \frac{1}{\tau_r}\cdot\left(i_{ds} - i_{ds}^*\right)\ . \tag{21}$$

Due to the fact that i_{ds} is not a control input, an error variable $z_2 = i_{ds} - i_{ds}^*$ is defined and we have the derivative as follows:

$$\dot{z}_2 = c_1 \cdot z_1 + \frac{1}{\tau_r}\cdot z_2\ . \tag{22}$$

Step 2:

The derivative of the error variable $z_2 = i_{ds} - i_{ds}^*$ is:

$$\dot{z}_2 = -\frac{L_m}{\tau_r}\cdot\left(L_m \cdot i_{ds} - \phi_{dr}\right) + c_1 \cdot \left(i_{ds} - \frac{\phi_{dr}}{L_m} - \tau_r \cdot \frac{d\phi_{dr}^*}{dt}\right) -$$
$$\frac{\tau_r}{L_m}\cdot\frac{d^2\phi_{dr}}{dt^2} + \frac{1}{\sigma \cdot L_s}\cdot V_{ds} - \tag{23}$$
$$\frac{1}{\sigma \cdot L_s}\left(R_r \cdot i_{ds} - w_e \cdot \sigma \cdot L_s \cdot i_{qs} + \left(\frac{L_m}{L_r}\right)^2 \cdot R_r \cdot \left(i_{ds} - \frac{\hat{\phi}_{dr}}{L_m}\right)\right) +$$
$$\frac{\left(\frac{L_m}{L_r}\right)^2 \cdot R_r}{\sigma \cdot L_s}\cdot\frac{\phi_{dr}}{L_m} + w_r \cdot \frac{L_m}{\sigma \cdot L_s \cdot L_r}\cdot\phi_{qr}\ .$$

Viewing ϕ_{dr} and ϕ_{qr} as unknown disturbances, we apply nonlinear damping [13, 17] to design the control function:

$$\frac{1}{\sigma\cdot L_s}\cdot V_{sd}=\frac{1}{\sigma\cdot L_s}\left(R_s\cdot i_{ds}-w_e\cdot\sigma\cdot L_s\cdot i_{qs}+\left(\frac{L_m}{L_r}\right)^2\cdot R_r\cdot\left(i_{ds}-\frac{\hat{\phi}_{dr}}{L_m}\right)\right)$$
$$\left(\frac{1}{\tau_r}-c_1\right)\cdot\left(i_{ds}-\frac{\hat{\phi}_{dr}}{L_m}\right)+$$
$$c_1\frac{\tau_r}{L_m}\cdot\frac{d\phi^*_{dr}}{dt}+\frac{\tau_r}{L_m}\cdot\frac{d^2\phi^*_{dr}}{dt^2}\qquad(24)$$
$$-c_2\cdot z_2-\frac{1}{\tau_r}\cdot z_1-d_2\cdot$$
$$\left\{\left(\frac{(L_m/L_e)^2R_r}{\sigma L_s}\right)^2+\left(w_r\cdot\frac{(1-\sigma)}{\sigma}\right)^2\right\}\cdot z_2\ .$$

We define:

$$\phi_1=\frac{\left(\frac{L_m}{L_r}\right)^2\cdot R_r}{\sigma\cdot L_s},\ \phi_2=w_r\cdot\frac{\frac{L_m^2}{L_r}}{\sigma\cdot L_s}\ \text{and}\ \phi^2=\phi_1^2+\phi_2^2\ .$$

The insertion of the control function in the dynamics for the error variable z_2 gives :

$$\dot{z}_2=-c_2\cdot z_2-\frac{1}{\tau_r}z_1-d_2\cdot\phi^2\cdot z_2+\phi_1\cdot\frac{\phi_{dr}}{L_m}+\phi_2\cdot\frac{\phi_{qr}}{L_m}.\qquad(25)$$

Step 3:

We now search to find the error torque tracking. A tracking error for $\phi_{dr}\neq 0$ is defined as:

$$z_3=i_{qs}-\frac{T_e^*}{\left(P\cdot\frac{L_m}{L_r}\cdot\phi_{dr}\right)}.\qquad(26)$$

Then, its derivative is:

$$\dot{z}_3=\frac{1}{\sigma\cdot L_s}\cdot V_{qs}-\frac{1}{\sigma\cdot L_s}\cdot\left(R_s\cdot i_{sq}+w_e\cdot\sigma\cdot L_s\cdot i_{ds}+\left(\frac{L_m}{L_r}\right)^2\cdot R_r\cdot i_{qs}+w_r\cdot(1-\sigma)\cdot L_s\cdot\frac{\hat{\phi}_{dr}}{L_m}\right)-\frac{\left(\frac{L_m}{L_r}\right)^2\cdot R_r}{\sigma\cdot L_s}\cdot\frac{\phi_{qr}}{L_m}+\qquad(27)$$
$$w_r\cdot\frac{\frac{L_m^2}{L_r}}{\sigma\cdot L_s}\cdot\frac{\phi_{dr}}{L_m}+\frac{L_r\cdot T_e^*}{P\cdot\phi_{dr}^2}\cdot\frac{1}{\tau_r}\cdot\left(i_{ds}-\frac{\hat{\phi}_{dr}}{L_m}\right)-\frac{L_r}{P\cdot L_m\cdot\hat{\phi}_{dr}}\cdot\frac{dT_e^*}{dt}.$$

Viewing ϕ_{dr} and ϕ_{qr} as unknown disturbances, we apply nonlinear damping [13, 17] to design the control function:

$$\frac{1}{\sigma\cdot L_s}\cdot V_{qs}=\frac{1}{\sigma\cdot L_s}\cdot\left(R_s\cdot i_{qs}-w_e\cdot\sigma\cdot L_s\cdot i_{qs}+\left(\frac{L_m}{L_r}\right)^2\cdot R_r\cdot i_{qs}+w_r\cdot(1-\sigma)\cdot L_s\cdot\frac{\hat{\phi}_{dr}}{L_m}\right)-\frac{2\cdot L_r\cdot T_e^*}{3\cdot P\cdot\phi_{dr}}\cdot\frac{1}{T_r}\cdot\left(i_{ds}-\frac{\hat{\phi}_{dr}}{L_m}\right)+\qquad(28)$$
$$\frac{2\cdot L_r}{3\cdot P\cdot L_m\cdot\hat{\phi}_{dr}}\cdot\frac{dT_e^*}{dt}-c_3\cdot z_3-d_3\cdot\left\{\left(\frac{\left(\frac{L_m}{L_r}\right)^2\cdot R_r}{\sigma\cdot L_s}\right)^2+\left(w_r\cdot\frac{(1-\sigma)}{\sigma}\right)^2\right\}\cdot z_3\ .$$

The insertion of the control function in the dynamics for the error variable z_3 then gives:

$$\dot{z}_3=-c_3\cdot z_3-d_3\cdot\phi^2\cdot z_3+\phi_1\cdot\frac{\phi_{qr}}{L_m}+\phi_2\cdot\frac{\phi_{dr}}{L_m}\ .\qquad(29)$$

The combined controller is shown in Figure 2 where we have:

$$\begin{cases}V_{ds,ff}=R_s\cdot i_{ds}-\omega_s\cdot\sigma\cdot L_s\cdot i_{qs}+\left(\frac{L_m}{L_r}\right)^2\cdot R_r\cdot\left(i_{ds}-\frac{\hat{\phi}_{dr}}{L_m}\right)\\ V_{qs,ff}=R_s\cdot i_{sq}-\omega_s\cdot\sigma\cdot L_s\cdot i_{qs}+\left(\frac{L_m}{L_r}\right)^2\cdot R_r\cdot i_{sq}+\omega_r\cdot(1-\sigma)\cdot L_s\cdot\frac{\hat{\phi}_{dr}}{L_m}\\ V_{ds,nl}=\sigma\cdot L_s\cdot\left\{\left(\frac{1}{\tau_r}-c_1\right)\cdot\left(i_{ds}-\frac{\hat{\phi}_{dr}}{L_m}\right)-\frac{1}{L_m\cdot\tau_r}\left(\hat{\phi}_{dr}-\phi^*_{dr}\right)\right\}\\ V_{qs,nl}=-\frac{2\cdot L_m^2\cdot T^*_{em}}{3\cdot P\cdot(1-\sigma)\cdot L_s\cdot\phi^2_{dr}}\cdot\frac{\sigma\cdot L_s}{\tau_r}\cdot\left(i_{ds}-\frac{\hat{\phi}_{dr}}{L_m}\right)\end{cases}\qquad(30)$$

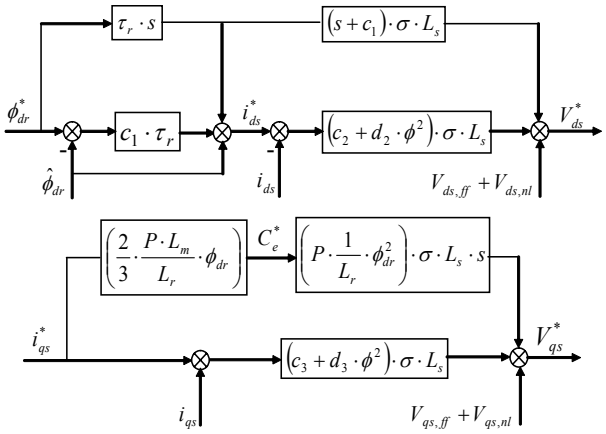

Figure 2. Nonlinear field-oriented control of IM using Backstepping technique

c) Speed control of IM using backsteping

To control the speed of the induction motor, we look to search the error speed tracking. We consider that i^*_{qs} is the control law, so the tracking error is defined as:

$$z_0 = \omega_r^* - \omega_r . \quad (36)$$

So, its derivate is given as :

$$\dot{z}_0 = \dot{\omega}_r^* - \dot{\omega}_r , \quad (37)$$

$$\dot{z}_0 = \dot{\omega}_r^* - \left[\frac{3}{2} \frac{P^2 \cdot L_m}{L_r \cdot J} \cdot i_{qs} \cdot \phi_{dr} - \frac{f_c}{J} \cdot \omega_r - \frac{P}{J} \cdot T_l \right] . \quad (38)$$

The control law obtained is :

$$i_{qs}^* = \frac{2}{3} \frac{L_r \cdot f_c}{P^2 \cdot L_m \cdot \phi_{dr}} \cdot \omega_r + c_0 \frac{2 \cdot L_r \cdot J}{3 \cdot P^2 \cdot L_m \cdot \phi_{dr}} z_0 + \frac{2}{3} \frac{L_r}{P \cdot L_m} \cdot T_l . \quad (39)$$

4. Fuzzy rotor resistance estimation

In this section, the fuzzy rotor resistance estimation is proposed. The first challenge in the design of this fuzzy logic estimator is to determine its input variables. Since the time constant for the variation of the rotor resistance is much larger than the time constant of the IM, the rotor resistance estimation process can be running under steady-state conditions (no changes of load torque and reference speed command).

Because of the variation of R_r and L_r, the desired field-orientation conditions (Eq. (6) to (8)) can not always be maintained and the drive performance can be significantly affected. For the normal operation of the drive and without considering the effects derived from the saturation (L_r), this rotor resistance can change up to 200% over operation.

In order to study the influence of the rotor resistance, a characteristic function *F* is utilized [5, 6]:

$$F = \frac{1}{\omega_r \omega_e} \left[\left(V_{ds} - \sigma L_s \frac{di_{sd}}{dt} \right) i_{sq} - \left(V_{qs} - \sigma L_s \frac{di_{sq}}{dt} \right) i_{sd} \right] + \sigma L_s \left(i_{sd}^2 + i_{sq}^2 \right) . \quad (40)$$

This function can also be defined from a modified expression of field orientation conditions as follows:

$$F = \frac{L_m}{L_r} \left(\frac{d\phi_{rd}}{dt} i_{sq} - i_{sd} \cdot \phi_{rd} \right) . \quad (41)$$

In steady state $\left(\frac{d\phi_{rd}}{dt} = 0 \right)$, this equation becomes:

$$F_0 = -\frac{L_m}{L_r} i_{sd} \cdot \phi_{rd} . \quad (42)$$

Note that the function given in Eq. (42) differs from *F* by the effect of change of R_r [7]. In fact, the rotor resistance used in flux estimator is not actual value of R_r unless a rotor resistance adaptation is present. The error (F-F_0) reflects the rotor resistance variation, and can be used as a correction function for the adaptation of the rotor resistance in the fuzzy logic estimator.

The proposed estimator based on fuzzy logic principle is shown in Figure 5. Functions F_0 and F are first calculated. The error between F and F_0 (ΔF) and its first time derivative are submitted as inputs to FLE. The operation principle of FLE is similar as of a fuzzy logic controller (FLC). The membership functions for the fuzzy sets corresponding to the error ΔF, its time variation and incremental rotor resistance ΔR_r are defined in Figures 3 and 4.

Because the data manipulated in the fuzzy inference mechanism is based on the fuzzy set theory, the associated fuzzy sets involved in the fuzzy control rules are defined as follows:

NB : Negative big
NM : Negative medium
NS : Negative small
ZE : Zero
PS : Positive small
PM : Positive medium
PB : Positive big

And their universe of discourses are assigned to be between [-1, 1] for the inputs (ΔF and its time variation), and [-1,1] for the output variable (ΔR_r). The incremental rotor resistance ΔR_r is continuously added to the previously estimated rotor resistance R_{r0}.

Since only seven fuzzy subsets, NB, NM, NS, ZE, PS, PM and PB, are defined for ΔF, its time variation and ΔR_r, the fuzzy inference mechanism contains 49 rules. The resulting fuzzy inference rules for the incremental rotor resistance are as follows:

	NB	NM	NS	ZE	PS	PM	PB
NB	NB	NB	NB	NB	NB	NM	ZE
NM	NB	NB	NB	NM	NS	ZE	PS
NS	NB	NB	NM	NS	ZE	PS	PM
ZE	NB	NM	NS	ZE	PS	PM	PB
PS	NM	NS	ZE	PS	PM	PB	PB
PM	NS	ZE	PS	PM	PB	PB	PB
PB	ZE	PS	PS	PB	PB	PB	PB

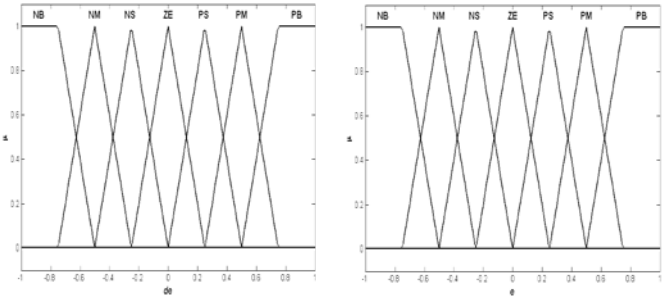

Figure 3. Membership functions for antecedent part

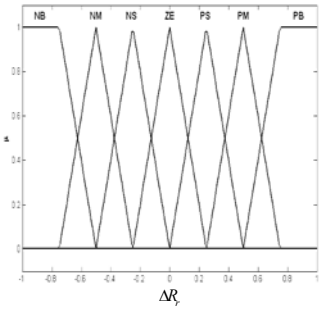

Figure 4. Membership functions consequent part

Finally, the fuzzy output ΔR_r can be calculated by the centre of area defuzzification as:

$$\Delta R_r = \frac{\sum_{i=1}^{7} w_i c_i}{\sum_{i=1}^{7} w_i} = \frac{\begin{bmatrix} c_1 & \cdots & c_7 \end{bmatrix} \begin{bmatrix} w_1 \\ \vdots \\ w_7 \end{bmatrix}}{\sum_{i=1}^{9} w_i} = \upsilon^T W \quad (43)$$

where $\upsilon = \begin{bmatrix} c_1 & \cdots & c_7 \end{bmatrix}$, c_1 trough c_7 are the centre of the membership functions of ΔR_r and $W = \begin{bmatrix} w_1 & \cdots & w_7 \end{bmatrix} \Big/ \sum_{i=1}^{7} w_i$ is firing strength vector.

The simulated value of R_r is used in the slip calculation (6) and rotor flux estimator (8) as shown in Figure 6 to ensure the correct operation of induction motor control.

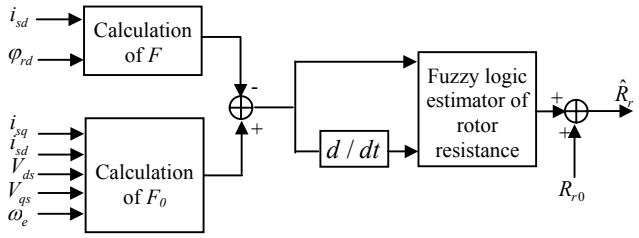

Figure 5. Block diagram of rotor resistance estimation using fuzzy logic

5. Results of simulation

To prove the rightness and effectiveness of the proposed control scheme, we apply the designed controller to the control of the induction motor. The induction motor is a wound three phase, *Y* connected, four pole, 1.5 kW, 1420min^{-1} 220/380V, 50Hz. The machine parameters are given in the appendix. The configuration of the overall control system is shown in Figure 6. It mainly consists of an induction motor, a ramp comparison current-controlled pulse width modulated (PWM) inverter, a slip angular speed estimator, an inverse park, nonlinear filed oriented control based on backstepping technique, and an outer speed feedback control loop contains on a backstepping controller.

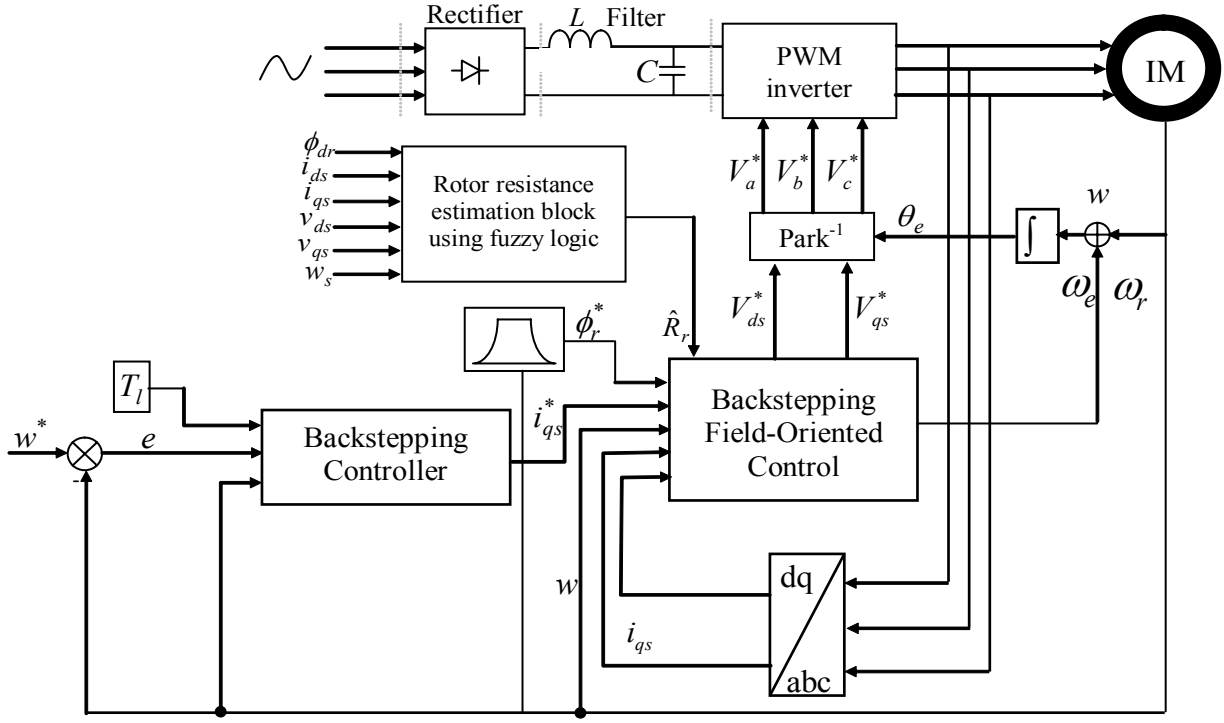

Figure 6. Block of the speed control and field oriented control of IM using backstepping technique with fuzzy rotor resistance estimator

Figure 7 shows the disturbance rejection of backstepping controller when the machine is operated at 200 [rad/sec] under no load and a nominal load disturbance torque (10 N.m) is suddenly applied and eliminated at 1.5sec, 2.5sec respectively, followed by a reversed reference (-200rad/sec) at 4sec. The backstepping controller rejects the load disturbance rapidly with a negligible steady state error.

This controller rejects the load disturbance very quickly with no overshoot and with a negligible steady state error more than the PI controller which is shown clearly in Figures 11 and 12. The PI controller parameters are selected in an optimal way using the poles placement method. The proportional and the integral constant are given as follow: k_p = 1.5574, k_i = 10.044. The constants c_i , $i = 0,1,2,3$ of the backstepping control strategy, which indicate the speed of convergence for the state variable (rotor speed w_r) are chosen as $c_0 = 18$, $c_1 = 5.5$, $c_2 = 7.5$, $c_3 = 7.5$.

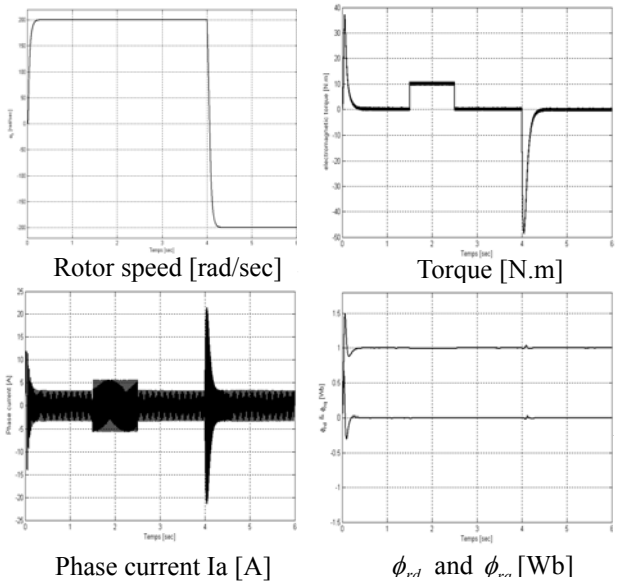

Figure 7. Simulated results of backstepping controller for IM

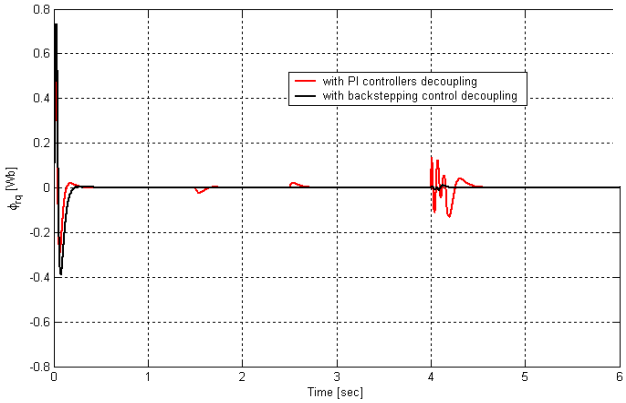

Figure 8. Simulated results of the comparison between the decoupling obtained by PI and backstepping design for IM

Figures 8 and 9 show a comparison between the classical field oriented control using PI controller and that based on the backstepping design technique. They show clearly that the decoupling control is more maintained for the backstepping design than that obtained by a classical PI controllers (current and flux regulators).

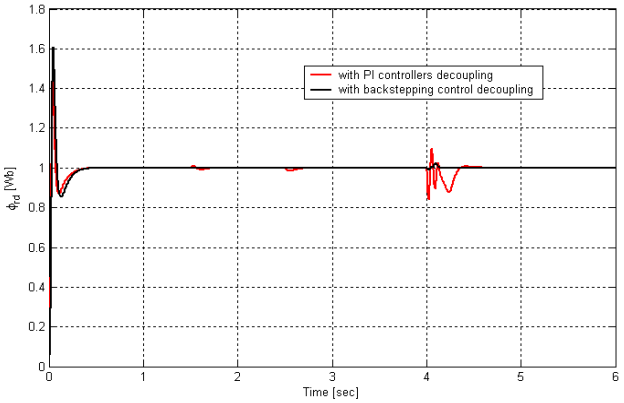

Figure 9. Simulated results of the comparison between the decoupling obtained by PI and backstepping design for IM

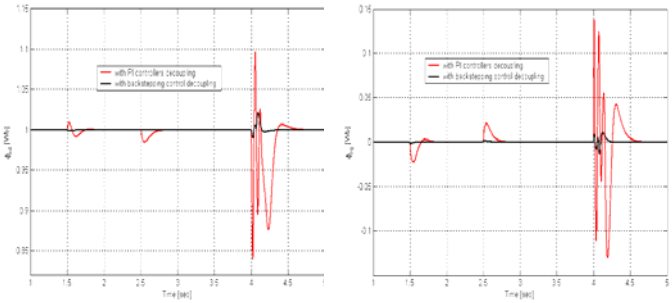

Figure 10. Zoomed responses of decoupling obtained by PI, backstepping control for IM

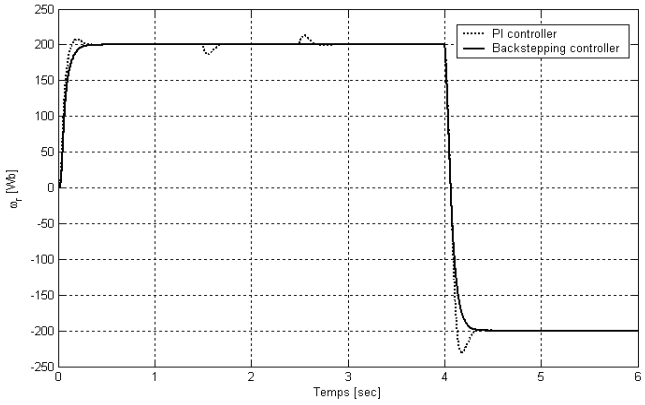

Figure 11. Simulated results of the comparison between the PI and backstepping design for IM speed control

In the next simulation, the rotor resistance is supposed to be changed from 100% of its rated value to 200% linearly (step or ramp change). The responses of direct and quadratic rotor flux for the two cases (without and with rotor resistance adapting) and for step change are shown in Figure 13. It's observed in these figures that when the estimated rotor resistance deviates from its real value, the field orientation scheme is detuned. Figure 13 shows also the main-

tained performance of the IM drive using the rotor resistance adaptation to track its real value. In this case, the field orientation condition can be maintained by applying a step change of rotor resistance. It's observed that the detuned problem is removed completely ($\phi_{rd} = \phi_r$ and $\phi_{rq} = 0$).

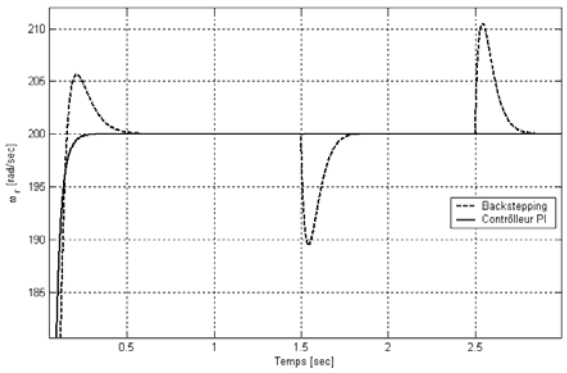

Figure 12. Zoomed responses of speed control obtained by PI, backstepping control for IM

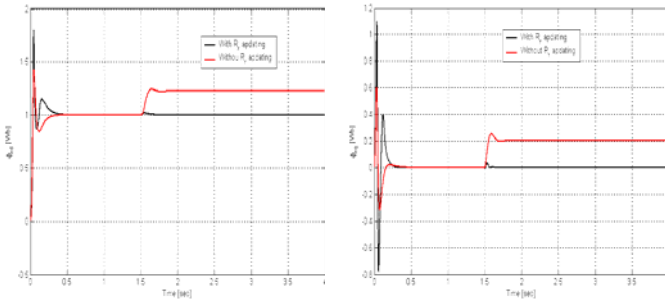

Figure 13. Simulated results of the direct and quadratic flux without and with rotor resistance adaptation (step change)

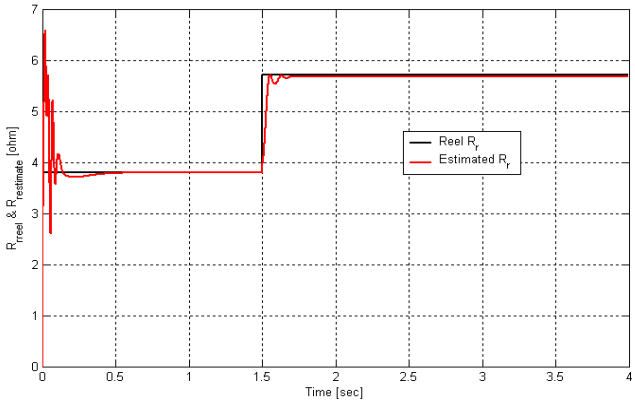

Figure 14. Rotor resistance tracking for step change

Figure 15 shows the responses of the direct and quadratic rotor flux with and without adaptation, for ramp change of rotor resistance. The same remarks can be observed for the responses shown in Figure 13. Finally, Figures 14 and 16 show the rotor resistance tracking for step and ramp change. In both cases, the rotor resistance tracking is excellent and the field orientation condition is still maintained. We can analyze finally the principle of the obtained results for rotor resistance adaptation. If the system is under noload condition, the torque current becomes zero. The calculated function F and F_0 are not affected by the rotor resistance change. This is shown in Figure 13 and Figure 15 from 0 sec until 1.5 sec. However, if the load is added to the motor, the rotor resistance errors will affect the calculated functions.

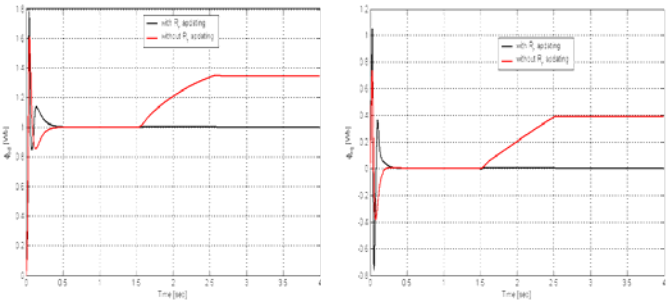

Figure 15. Simulated results of the direct and quadratic flux without and with rotor resistance adaptation (ramp change)

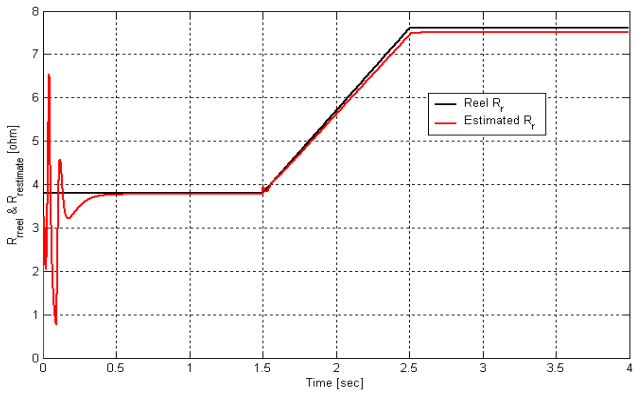

Figure 16. Rotor resistance tracking for ramp change

The figures show that the proposed scheme achieves good performances as it achieves compensation of the rotor resistance changes.

6. Conclusion

In this work, we have presented a backstepping technique associated with fuzzy rotor resistance estimation in order to offer a choice of design tools to accommodate uncertainties and nonlinearities. This study has successfully demonstrated the design of the backstepping technique for the speed control of an induction motor and the nonlinear field orientation control design. The proposed scheme has presented satisfactory performances (no overshoot, minimal rise time, best disturbance rejection) for parameter variations, time-varying external force disturbances. The proposed fuzzy rotor resistance estimator produces a correction signal which is added to the rated value of the rotor resistance. The simulation results obtained have confirmed the excellent flux responses and the efficiency of the proposed scheme. Finally, the effectiveness of the PI controller and the nonlinear field orientation based on the backstepping strategy has been verified through simulation.

Appendix

Induction motor parameters:

P_n [kW]	1.5	R_s [Ω]	4.85	f_n [Hz]	50
V_n [V]	220	R_r [Ω]	3.805	J_n [kg/m^2]	0.031
η	0.78	L_r [H]	0.274	f_c [N.m.s/rd]	0.0014
Cosφ_n	0.8	L_s [H]	0.274	p	2
ω_n[min^{-1}]	1428	L_m [H]	0.258		

References

[1] **J.P. Caron, J.P. Hautier.** Modeling and Control of Induction Machine. *Technip Edition* (1995) (*text in french*).

[2] **A. Hazzab, I. K. Bousserhane, M. Kamli, M. Rahli.** Design of fuzzy sliding mode controller by genetic algorithms for induction machine speed control. *Third IEEE International Conference on Systems, Signals & Devices SSD'05*, Tunisia, 2005.

[3] **A. Hazzab, I.K. Bousserhane, M. Kamli, M. Rahli.** New Adaptive fuzzy PI-Sliding Mode Controller for Induction Machine Speed Control. *Third IEEE International Conference on Systems, Signals & Devices SSD'*05, Tunisia, 2005.

[4] **R.D. Lorenz, D.B. Lawson.** A Simplified Approach to Continuous On-Line Tuning of Field-Oriented Induction Machine Drives. *IEEE Trans. On Industry application*, *Vol*.26, *Issue* 3, *May*/*June* 1990.

[5] **Y. Miloud, A. Draou**. Performance Analysis of a Fuzzy Logic Based Rotor Resistance Estimator of an Indirect Vector Controlled Induction Motor Drive. *Turk. Jour. Elec. Engin. Vol*.13, *No*.03, 2005.

[6] **T.–C. Minh, L.–H. Hoang.** Model Reference Adaptive Fuzzy Controller and Fuzzy Estimator for High Performance Induction Motor Drives. *Thirty First IEEE IAS Annual Meeting Conference Record, Vol*.1, 1996, 380-387.

[7] **B. Karanayil, M. F. Rahman, C. Grantham.** PI and Fuzzy Estimators for On-line Tracking of Rotor Resistance of Indirect Vector Controlled Induction Motor Drive. *IEEE Inter. Conf. on Power Electronics,* 2001.

[8] **R.–J. Wai, D.–C. Liu, F.–J. Lin**. Rotor Time Constant Estimation Approaches Based on Energy Function and Sliding Mode for Induction Motor Drive. *Electric Power Sytem Research*, *Vol*.52, 1999, 229-239.

[9] **L. Baghli.** Contribution to Induction Machine Control: Using Fuzzy Logic, Neural Networks and Genetic Algorithms. *Doctoral Thesis, Henri Poincare University*, *January* 1999 (*text in french*).

[10] **M.A. Ouhrouche, C.Volet.** Simulation of a Direct Field-Oriented Controller for an Induction Motor Using Matlab/Simulink Software Package. *Proc. of IASTED Int. Conf. Modeling and Simulation (MS'*2000*)*, *USA*.

[11] **I. Kanellakopoulos, P.V. Kokotovic, A.S. Morse.** Systematic design of adaptive controller for feedback linearizable systems. *IEEE Trans., Auto. Control*. 1991. 36. (11), 1241- 1253.

[12] **F.J. Lin, C.C. Lee.** Adaptive backstepping control for linear induction motor drive to track period refernces. *IEE Proc. Electr. Power Appl.*, 2000,147, (6), 449-458.

[13] **H. Rasmussen, P. Vadstrup, H. Borsting.** Nonlinear decoupling of Torque and Field Amplitude of Induction Motors. *FINPIE/97 Espoo* Finland, 1997.

[14] **T. Yaolong, J. Chang, T. Hualin.** Adaptive Backstepping Control and Friction Compensation for AC Servo with Inertia and Load Uncerainties. *IEEE Trans. On Ind. Elect*. *Vol*.50, *No*.5, 2003.

[15] **J. Jung, K. Nam.** A Dynamic Decoupling Control Scheme for High-Speed Operation of Induction Motors. *IEEE Trans. on Ind. Elect., Vol*.46/01, 1999.

[16] **LI Zhen, Longya Xu.** On-Line Fuzzy Tuning of Indirect Field-Oriented Induction Machine Drives. *IEEE Trans. on Power Electronics*, *Vol*.13, *No*.1, 1998.

[17] **A.R. Benaskeur.** Aspects de I'application du backstepping adaptatif à la commande décentralisée des systèmes non-linéaires'. *PhD thesis, Department of Electrical and Computer Engineering, Universite Laval*, Quebec City, Canada, 2000.

[18] **M. Krstié, I. Kanellekapolous, P.V. Kokotovic.** Nonlinear Design of Adaptive Controllers for Linear Systems. *IEEE Trans. Automat. Contr.*, *Vol*.39, 1994, 738-752.

Received August 2006.

DOI: 10.5755/j01.itc.35.4.11781